



International Journal for Innovative Engineering and Management Research

A Peer Reviewed Open Access International Journal

www.ijiemr.org

COPY RIGHT



ELSEVIER
SSRN

2019IJIEMR. Personal use of this material is permitted. Permission from IJIEMR must be obtained for all other uses, in any current or future media, including reprinting/republishing this material for advertising or promotional purposes, creating new collective works, for resale or redistribution to servers or lists, or reuse of any copyrighted component of this work in other works. No Reprint should be done to this paper, all copy right is authenticated to Paper Authors

IJIEMR Transactions, online available on 4th Feb 2019. Link :

<http://www.ijiemr.org/main/index.php?vol=Volume-08&issue=ISSUE-02>

Title: **A FAST MULTIPLE-IMAGES DEHAZING METHOD BASED ON A PIXEL MODEL AND GRAY PROJECTION**

Volume 08, Issue 02, Pages: 1–8.

Paper Authors

RAMESH REDDY, P. BHANU PRAKASH REDDY

Vaishnavi Institute of Technology, Tirupati, AP, India



USE THIS BARCODE TO ACCESS YOUR ONLINE PAPER

To Secure Your Paper As Per **UGC Guidelines** We Are Providing A Electronic Bar Code



A FAST MULTIPLE-IMAGES DEHAZING METHOD BASED ON A PIXEL MODEL AND GRAY PROJECTION

RAMESH REDDY, P. BHANU PRAKASH REDDY

Dept of ECE, Vaishnavi Institute of Technology, Tirupati, AP, India.

rameshreddy80089@gmail.com

ABSTRACT Due to the scattering of atmospheric particles, pics captured underneath hazy situations suffer from comparison attenuation and shade distortion, which critically affect the overall performance of device imaginative and prescient systems. Various kinds of methods were advanced to enhance the clarity of photographs. However, those techniques are usually challenging to apply in actual-time structures. We present a fast, single-photo dehazing method primarily based on the atmospheric scattering idea and darkish channel prior principle. The transmission map is about expected using a quick common filter, the subsection mechanism is designed to keep away from the high brightness of the sky area in the recovered photograph, the location projection approach is followed to acquire the atmospheric light, and image shade repayment is implemented the use of the Weber_Fechner regulation. Our experimental consequences display that this set of rules can restore pictures to a clean and natural state and make certain the stability of high-quality and the speed of picture healing. Therefore, the set of rules may be utilized in real-time systems.

Keywords:- Gray projection, image dehazing, subsection mechanism, transmission estimation.

I. INTRODUCTION

In hazy conditions, the scattering of atmospheric particles leads to severe degradation of the information captured by optical sensors. The contrast and fidelity of the image are attenuated to different degrees, which directly affects the visual perception of human operators and the performance of the machine vision system [1], [2]. Therefore, it is important to investigate methods of image dehazing. Generally, such methods are divided into the image-enhancement-based method and image-restoration-based method. The first class aims to improve the image visual effects by enhancing the contrast of hazy images, including histogram equalization

[3], Retinex [4], homomorphic filtering [5], and wavelet transform [6], among other methods. These methods can enhance the visual effect of the image but do not reliably remove the haze. In the image-restoration-based method, a physical model is established for the degradation of the hazy image, and the lost information is compensated with the inversion algorithm. This method has the natural effect of dehazing and has received considerable recent attention [7]. For example, Narasimhan and Nayar [8] obtained approximate depth information by artificially specifying the maximum and the minimum depth of field. They then

recovered a clear image based on the physical model. Hautiere *et al.* [9] used a vehicle-mounted optical sensor system to calculate the depth of the scene and applied a 3-D geography model to dehaze the images. Kopf *et al.* [10] used a map to provide the basic terrain, constructed a 3-D model of the scene from known depth and texture information, and then used a model to achieve dehazing. This method is based on the premise that depth information for the scene is known and can be used to perform reliable image restoration. Subsequently, Schechner *et al.* [11] used the polarization characteristics of sky brightness to capture multiple images of the same scene at different polarization angles and then reconstructed the degraded image with depth information by estimating the degree of polarization. Nayar and Narasimhan [12] obtained the depth information of a scene and restored the image by capturing two images in different weather conditions, which achieved satisfactory results. Both algorithms require multiple images for post processing, however, and it is often challenging to obtain multiple images of the same scene under different conditions in practice, hindering the application and popularization of these approaches.

In recent years, single image-dehazing algorithms based on a certain hypothesis or prior knowledge have garnered significant attention. For example, Tan [13] achieved image dehazing by maximizing the contrast of the restored image based on the prior knowledge that the haze-free image had a higher contrast than the hazy image. However, this approach can easily lead to oversaturation. Fattal [14] assumed that the

surface chromaticity of the object was not statistically correlated with the propagation of the medium and used independent component analysis to estimate the albedo of the scene. This method can produce satisfactory results when the haze is thin but fails for thick hazy images because of the lack of color information. He *et al.* [15] proposed a dehazing method based on the dark channel prior (DCP). This process uses a minimum filter to estimate and optimize the transmission map of the media, which is designed from the statistics of a haze-free image database and achieves satisfactory results. Tarel and Hautière [16] used a median filter to estimate the atmospheric transmission function and then applied a tone map to obtain the dehazed image. The algorithm recovered the image clearly and vividly but caused a halo effect from the depth-of-field mutation. Kratz and Nishino [17] assumed that the hazy image was composed of two separate layers: the scene albedo and the scene depth. They ultimately achieved relatively accurate depth information using the factorial Markov random field (FMRF). However, the color in the image obtained by this method was too saturated. Subsequently, Ancuti and Ancuti [18] proposed a method based on image fusion, Wang and Feng [19] proposed a dehazing algorithm based on transmittance fusion, Gibson and Nguyen [20] presented a fast, single-image dehazing algorithm using adaptive Wiener filtering, Meng *et al.* [21] proposed an efficient regularization method for single-image dehazing, Kim *et al.* [22] proposed a cost function method based on image contrast and the degree of lost information, Fattal [23] proposed a

colorbased method, and Zhu *et al.* [24] proposed a prior color attenuation to create a linear model. Among the above algorithms, the DCP method proposed by He *et al.* [15] has been widely investigated because of its simple principle and superior results. However, the method uses soft-matting to refine the transmission map, which requires high computational costs. A variety of methods have been developed to accelerate the transmission map refinement, such as bilateral filtering [25], [26], guided filtering [27], anisotropic filtering [28], edge-preservation filtering [29], and median filtering [30], which are challenging to implement in real-time systems [31]. In addition, the sky region and white objects do not meet the prior dark channel assumption, which results in a block effect or severe color distortion in the restored image. We propose an improved algorithm based on the DCP to address the fact that the current dehazing method is ineffective for sky regions and that the processing time is excessively long. The algorithm obtains the transmission map through a simple and fast average filtering process to improve the running speed. By segmenting the calculations, we eliminate block effects and color distortion. In addition, to address the phenomenon of image dimming after restoration, color remapping is performed to increase the visual effect of the image. The algorithm achieves a certain degree of dehazing and reduces the processing time, which has application value.

The remainder of this paper is organized as follows. Section 2 briefly introduces the atmospheric scattering model. In Section 3, the key steps are described, including the

principle of sky segmentation, the method to obtain atmospheric light using the quad-tree, the fusion principle of the transmission map and the method of image restoration. Section 4 presents the experimental results, and Section 5 concludes this work.

II. RELATED WORK

A. ATMOSPHERIC SCATTERING MODEL

According to the theory of atmospheric scattering, an imaging model of a hazy scene consists primarily of two parts, which is shown in Figure 1. The first part is the attenuation process of the rejected light from the object surface to the camera.

The second part is the scattering of air-light reaching the camera. Both parts constitute the theoretical basis of blurred hazy images.

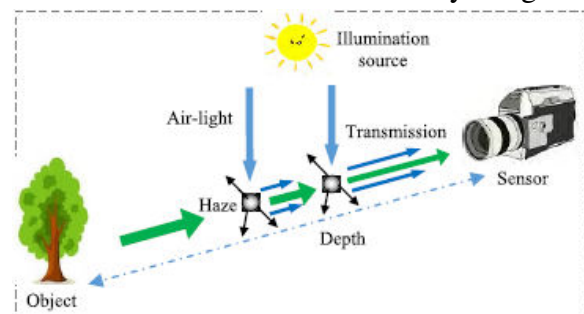


FIGURE 1. Atmospheric scattering model. Therefore, in the field of computer vision, the scattering model to describe hazy images can be expressed as

$$I(x) = J(x)t(x) + A(1 - t(x)) \quad (1)$$

where x is the distance coordinate, $I(x)$ is the hazy image, $J(x)$ is the haze-free image, A is the atmospheric light, and $t(x)$ is the transmission rate of the medium. The purpose of image dehazing is to recover $J(x)$ from $I(x)$.

The degradation model has several unknown parameters, resulting in an ill-posed problem. Only after estimating the

parameters A and $t(x)$ can $J(x)$ be restored from $I(x)$.

B. DCP THEORY

The DCP theory originates from the statistics of haze-free images [13]. That is, in most non-sky local regions, at least one color channel has a low value in some pixels that tend to zero, which can be expressed as follows:

$$J^{dark}(x) = \min_{c \in \{r, g, b\}} (\min_{y \in \Omega(x)} (J^c(y))) \rightarrow 0 \quad (2)$$

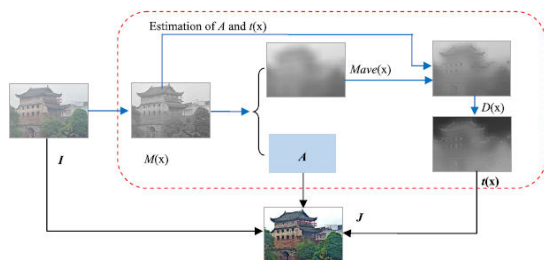


FIGURE 2. Framework of the image-dehazing algorithm.

where J^c is one color channel of J , $t(x)$ is a small block centered at x , and J^{dark} is the dark channel image. To estimate the transmission rate $t(x)$, we assume that the atmospheric light A is known and that the transmission rate $Qt(x)$ in the local region $\Omega(x)$ is constant. If both sides of Eq. (1) are simultaneously divided by A^c , then $\min_{c \in \{r, g, b\}} (\min_{y \in \Omega(x)} (J^c(y) / A^c))$ is transformed, and the $t(x)$ is obtained according to Eq. (2).

$$\tilde{t}(x) = 1 - \min_{c \in \{r, g, b\}} (\min_{y \in \Omega(x)} (\frac{J^c(y)}{A^c})) \quad (3)$$

In practice, to ensure that the image retains a sense of depth, a correction factor $w(0 < w < 1)$ is introduced to maintain partial haze. Then, Eq. (3) can be re-formulated as follows:

$$\tilde{t}(x) = 1 - w \min_{c \in \{r, g, b\}} (\min_{y \in \Omega(x)} (\frac{J^c(y)}{A^c})) \quad (4)$$

The block effect typically exists in the transmission map due to the assumption that the regional transmission is constant. Then, soft-matting or guided filtering [15] is used to refine $t(x)$. According to the atmospheric scattering model, once the transmission map $t(x)$ and the atmospheric light A are obtained, the scene depth can be restored according to Eq. (1):

$$J(x) = \frac{I(x) - A}{t(x)} + A \quad (5)$$

The estimation method of the atmospheric light A is to first select the top 0.1% of pixels with the largest brightness in J^{dark} and then to select the maximum value of the pixels that correspond to the pixels in the original image.

C. DEFECTS OF DCP

The algorithm proposed by He *et al.* [15] has the following limitations:

(1) The method uses soft-matting to refine the transmission map, which typically results in slow computing speed.

Although a variety of methods have been developed to accelerate the transmission map, refinements such as bilateral filtering [25], [26], guided filtering [27], anisotropic filtering [28], edge-preserving filtering [29], median filtering [30] and linear models [31] are still challenging to implement in real-time systems.

(2) The method cannot be applied to white regions, such as sky and water surfaces, due to the assumption of the DCP because the dark channel values of these regions $J^{dark}(x)$ are non-zero. That is,

$$t(x) = [1 - J^{dark}/A] < [1 - J^{dark}/A] / [1 - J^{dark}/A] \quad (6)$$

Thus, the transmission map estimated using the DCP-based algorithm is limited to the bright areas, which results in a signi_cant

enlargement of the slight difference between the pixel channels in the sky region after being divided by a relatively small t (as given by Eq. (4)). As a result, the color of the restored image is distorted.

III. FAST DEHAZING METHOD

To address the above problems, we designed a fast dehazing algorithm based on the DCP theory and gray projection in this paper. The algorithm reduces the operational complexity, ensures a successful dehazing effect, and can be applied to real-time systems. This method is divided into three steps.

(1) Estimation of the transmission map. Minimum filtering and fast average filtering are performed on the original image, and the white region is compensated by piecewise processing.

(2) Estimation of the atmospheric light. Gray projection is used to segment the sky region and calculate the atmospheric light.

(3) Image restoration. The atmospheric scattering model is used for image recovery, and the Weber-Fechner Law is selected to adjust the brightness. The entire process of the dehazing algorithm is shown in Figure 2.

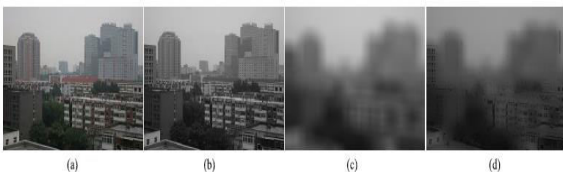


FIGURE 3. Estimation of transmission map. (a) Hazy image. (b) Minimum filtering. (c) Average filtering. (d) Grayscale optimization.

A. ESTIMATION OF TRANSMISSION MAP

The steps of the algorithm are as follows:

(1) Minimum Filtering To avoid the block effect caused by the transformation of Min

$c2fr;g;bg ()$ in the local region, the minimum of the three color channels is selected using the following formula:

$$M(x) = \min_{c \in \{r, g, b\}} (I^c(x)) \quad (7)$$

where x is a pixel in the image.

However, this calculation roughens the transmission map. As shown in Figure 3(b), the results are rich in edge information, and the luminance value does not accurately represent the haze density. Therefore, it is necessary to further eliminate the unnecessary texture information and the influence of white objects in $M(x)$.

(2) Fast Average Filtering

To smooth $M(x)$ and avoid the grayscale jump between neighboring pixels, average filtering is required, which is expressed as

$$M_{ave}(x) = average_{\lambda}(M(x)) \quad (8)$$

where λ is the size of the filter window, which is set at 1/20 of the image's width. To improve the computing speed [32], the integral image is used. For the input image i , the integral image $ii(x; y)$ at the pixel $(x; y)$ is defined as

$$ii(x, y) = \sum_{x' \leq x} \sum_{y' \leq y} i(x', y') \quad (9)$$

where $i(x', y')$ is the gray value of pixel (x', y') .

The sum of the pixels within an arbitrary rectangle can be obtained using the following operations:

$$ii(x, y) = ii(x-1, y) + ii(x, y-1) - ii(x-1, y-1) + i(x, y) \quad (10)$$

As shown in Figure 4, the integral image $ii(x; y)$ is equal to the sum of all the pixels in the gray portion of the image. Thus, for all pixels in a rectangular region D , the grayscale integral is

$$Sum(D) = i_4 + i_1 - (i_2 + i_3) \quad (11)$$

In this paper, a box filter is used to increase the calculation speed by a factor of four based on the integral image.

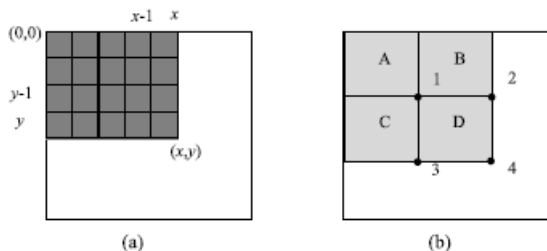


FIGURE 4. Calculation of the integral image. (a) Integral value of point (x; y). (b) Integral calculation of rectangle D.

In contrast, the data stored in the matrix are directly the sum of the current pixel and its neighbors. The corresponding element in the matrix can then be directly accessed, and the computational complexity is $O(1)$.

(3) Grayscale optimization. The result of the mean filtering can reflect the trend of the gray in the image. However, a gap remains within the real value that must be compensated as follows:

$$D(x) = \min(A \times M_{avg}(x), M(x)) \quad (12)$$

(4) If the atmospheric light A is known, then the transmission map can be calculated using Eq. (3). In practice, to retain a partial haze to give the image a sense of depth, the correction factor $w(0 < w < 1)$ is introduced. Then, Eq. (3) can be re-formulated as

$$\tilde{t}(x) = 1 - w \frac{D(x)}{A} \quad (13)$$

B. IMAGE RESTORATION AND TONE ADJUSTMENT

After the transmission map $t(x)$ and the atmospheric light A have been computed, the haze-free image of the scene under ideal conditions can be directly restored using Eq. (5).

When $t(x)$ approaches zero, the direct attenuation term also approaches zero. This relation excessively increases the dehazed image pixel values. The restored image may contain noise; thus, a lower bound t_0 is set for the transmission map $t(x)$, making the dehazing effects appear more natural.

The final dehazing image J is expressed as

$$J(x) = \frac{I(x) - A}{\max(t(x), t_0)} + A$$

In addition, since the image is affected by the surrounding environment and lighting on hazy days, parts of the images may have a low brightness, and the restored images based on the DCP will be even darker. According to the Weber-Fechner Law [35], the subjective brightness perceived by the human eye is acquired by nerve stimulation from light reflected from the object shining on the retina. The subjective brightness L_d and the objective brightness L_0 present a logarithmic linear relationship as follows:

$$J_d = \beta \lg(J) + \beta_0$$

where β and β_0 are constants. The relationship between the subjective brightness and the objective brightness is shown in Figure 8(a) and is used to adjust the tone of the restored images. To avoid the increased computation complexity from the logarithm operation, in the actual application of this method, a simple function is adopted to match Figure 8(a) with the following expression:

$$J_d = \frac{J(255 + k)}{J + k}$$

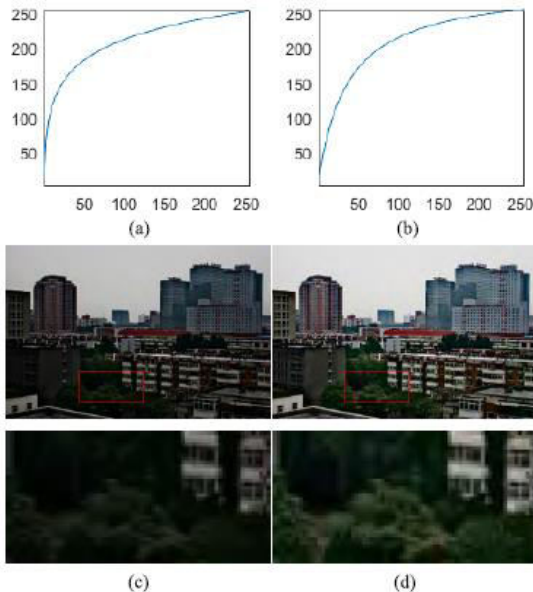


FIGURE 5. Adjustment curve of brightness.

(a) Weber-Fechner law. (b) Adjusted curve. (c) Before adjustment. (d) After adjustment. where k is the adjustment coefficient. The smaller the adjustment coefficient, the greater the degree of adjustment. The adjustment curve is shown in Figure 5(b) below. In the experiment, k is automatically obtained according to the average gray of the image, and its value is calculated using $k = 1.5 \times Im$. An image comparison before and after the adjustment is shown in Figure 5(c) and 5(d), where the lower images are the magnified areas of the rectangles. In Figure 5(c), although the haze is removed, the overall brightness is poor, giving the image a dark tone. Relative to Figure 5(c), the overall brightness and contrast of the adjusted image in Figure 5(d) is improved, and the visual effects are closer to the actual scene that would be seen under more favorable weather conditions.

IV. CONCLUSIONS

To improve the computational complexity of dehazing algorithms, a fast single-image dehazing method is proposed based on the

DCP theory and gray projection. The optimized average filtering method and box filter acceleration strategy are used to accommodate high-resolution and hazy images and videos in real-time systems. An atmospheric light acquisition method is designed based on the regional projection, and an amendment strategy for large white areas is proposed. Finally, an adaptive adjustment method based on human visual perception is proposed to solve the problem of low brightness in restored images. Relative to current state-of-the-art algorithms, it is concluded that the images restored from the proposed method appear clearer and more natural. The algorithm has a wide range of applicability to ensure the balance of quality and the speed of the image restoration and can be used in video systems. The key limitation of the proposed algorithm is that shadows appear at the edges of the dehazed image. Retaining the details and achieving edge smoothing is the subject of planned future work.

REFERENCES

- [1]. H. Lu *et al.*, "Depth map reconstruction for underwater Kinect camera using inpainting and local image mode filtering," *IEEE Access*, vol. 5, pp. 7115_7122, Apr. 2017.
- [2]. Y. Liu, H. Li, and M. Wang, "Single image dehazing via large sky region segmentation and multiscale opening dark channel model," *IEEE Access*, vol. 5, pp. 8890_8903, May 2017.
- [3]. T. K. Kim, J. K. Paik, and B. S. Kang, "Contrast enhancement system using spatially adaptive histogram equalization with temporal



- filtering," *IEEE Trans. Consum. Electron.*, vol. 44, no. 1, pp. 82_87, Feb. 1998.
- [4].T. J. Cooper and F. A. Baqai, "Analysis and extensions of the Frankle-McCann Retinex algorithm," *J. Electron. Imag.*, vol. 13, no. 1, pp. 85_92, Jan. 2004.
- [5].M.-J. Seow and V. K. Asari, "Ratio rule and homomorphic filter for enhancement of digital colour image," *Neurocomputing*, vol. 69, nos. 7_9, pp. 954_958, Mar. 2006.
- [6].S. Dippel, M. Stahl, R. Wiemker, and T. Blaffert, "Multiscale contrast enhancement for radiographies: Laplacian pyramid versus fast wavelet transform," *IEEE Trans. Med. Imag.*, vol. 21, no. 4, pp. 343_353, Apr. 2002.
- [7].J. P. Oakley and B. L. Satherley, "Improving image quality in poor visibility conditions using a physical model for contrast degradation," *IEEE Trans. Image Process.*, vol. 7, no. 2, pp. 167_179, Feb. 1998.
- [8].S. G. Narasimhan and S. K. Nayar, "Interactive (de) weathering of an image using physical models," in *Proc. IEEE Workshop Color Photometric Methods Comput. Vis.*, Paris, France, Oct. 2003, pp. 1_8.
- [9].N. Hautière, J.-P. Tarel, and D. Aubert, "Towards fog-free in-vehicle vision systems through contrast restoration," in *Proc. IEEE Conf. Comput. Vis. Pattern Recognit.*, Minneapolis, MN, USA, Jun. 2007, pp. 1_8.